




RESEARCH ARTICLE

Sister chromatid cohesion defects are associated with chromosomal copy number heterogeneity in high hyperdiploid childhood acute lymphoblastic leukemia

Larissa H. Moura-Castro¹  | Pablo Peña-Martínez¹  | Anders Castor² | Roman Galeev³ | Jonas Larsson³ | Marcus Järås¹ | Minjun Yang¹ | Kajsa Paulsson¹ 

¹Department of Laboratory Medicine, Division of Clinical Genetics, Lund University, Lund, Sweden

²Department of Pediatrics, Skåne University Hospital, Lund University, Lund, Sweden

³Division of Molecular Medicine and Gene Therapy, Lund Stem Cell Center, Lund University, Lund, Sweden

Correspondence

Dr. Kajsa Paulsson, Department of Laboratory Medicine, Division of Clinical Genetics, Lund University, BMC C13, SE-221 84 Lund, Sweden.

Email: kajsa.paulsson@med.lu.se

Funding information

Barncancerfonden, Grant/Award Numbers: PR2015-0012, TJ2016-0063; Cancerfonden, Grant/Award Number: CAN 2016/497; Crafoordska Stiftelsen, Grant/Award Number: 20180529; Governmental funding of clinical research within the National Health Service, Grant/Award Number: ALFSKANE-623431; Vetenskapsrådet, Grant/Award Number: 2016-01459

Abstract

High hyperdiploid acute lymphoblastic leukemia (ALL) is one of the most common malignancies in children. The main driver event of this disease is a nonrandom aneuploidy consisting of gains of whole chromosomes but without overt evidence of chromosomal instability (CIN). Here, we investigated the frequency and severity of defective sister chromatid cohesion—a phenomenon related to CIN—in primary pediatric ALL. We found that a large proportion (86%) of hyperdiploid cases displayed aberrant cohesion, frequently severe, to compare with 49% of *ETV6/RUNX1*-positive ALL, which mostly displayed mild defects. In hyperdiploid ALL, cohesion defects were associated with increased chromosomal copy number heterogeneity, which could indicate increased CIN. Furthermore, cohesion defects correlated with *RAD21* and *NCAPG* mRNA expression, suggesting a link to reduced cohesin and condensin levels in hyperdiploid ALL. Knock-down of *RAD21* in an ALL cell line led to sister chromatid cohesion defects, aberrant mitoses, and increased heterogeneity in chromosomal copy numbers, similar to what was seen in primary hyperdiploid ALL. In summary, our study shows that aberrant sister chromatid cohesion is frequent but heterogeneous in pediatric high hyperdiploid ALL, ranging from mild to very severe defects, and possibly due to low cohesin or condensin levels. Cases with high levels of aberrant chromosome cohesion displayed increased chromosomal copy number heterogeneity, possibly indicative of increased CIN. These abnormalities may play a role in the clonal evolution of hyperdiploid pediatric ALL.

KEYWORDS

acute lymphoblastic leukemia, aneuploidy, chromosomal instability, hyperdiploidy, sister chromatid cohesion

1 | INTRODUCTION

Changes in the number of chromosomes, termed aneuploidy, is one of the most common genetic aberrations in cancer cells. In spite of this,

many questions remain regarding its impact on the cell and its role in tumorigenesis. One such controversial issue is whether aneuploidy is always associated with chromosomal instability (CIN), that is an increased rate of missegregation of chromosomes at mitosis.¹

This is an open access article under the terms of the Creative Commons Attribution-NonCommercial-NoDerivs License, which permits use and distribution in any medium, provided the original work is properly cited, the use is non-commercial and no modifications or adaptations are made.

© 2020 The Authors. *Genes, Chromosomes & Cancer* published by Wiley Periodicals LLC.

The high hyperdiploid (HeH; 51-67 chromosomes) subgroup of B-cell precursor acute lymphoblastic leukemia (BCP ALL) comprises 25% to 30% of all pediatric cases and is associated with young age (3-5 years) at diagnosis and a superior prognosis.² Genetically, HeH leukemia is characterized by a specific aneuploidy, comprising gains of chromosomes X, 4, 6, 10, 14, 17, 18 and 21, which is believed to be the main driver event because it occurs very early in leukemogenesis and is always present in all leukemic cells.³⁻⁷ In contrast to many other aneuploid malignancies, there is little evidence for CIN in HeH ALL; extra chromosomes are rarely subclonal and the chromosomal pattern generally does not change over the course of the disease.^{3,6,8,9} Thus, HeH ALL appears to be a chromosomally stable aneuploid disease, suggesting that aneuploidy is not necessarily associated with CIN per se. However, underlying CIN that is masked by stable dividing major clones cannot be excluded.

We recently reported that HeH childhood BCP ALL displays relatively low expression of cohesin.¹⁰ Cohesin is a ring-like multi-protein complex that includes SMC1/SMC3 heterodimers, RAD21, and a STAG1 or STAG2 subunit.^{11,12} One of its main functions is to mediate sister chromatid cohesion at metaphase; a process that, if disrupted, may cause CIN.¹ Individuals with constitutional mutations in cohesin components, which cause Cornelia de Lange syndrome, have increased levels of cohesion defects¹³ and knockdown experiments in human cell lines have shown that loss of expression of *SMC1A*, *SMC3*, *STAG2*, and *RAD21* are all associated with cohesion defects to different degrees.¹⁴⁻²² In cancer, mutations in components of the cohesin complex are recurrent in a wide variety of malignancies, including acute myeloid leukemia, but conflicting results have been reported regarding their link to cohesion defects and aneuploidy.²³⁻²⁷ In line with this, a recent study has shown that primary HeH ALL cases present chromatid cohesion defects in addition to delays in early mitosis and chromosome-alignment defects.²⁸ The authors found an association between such aberrations and defective condensin complexes, aurora B kinase and the spindle assembly checkpoint²⁸ but did not address the possible link with cohesin levels.

In this study, we have investigated the severity and frequency of aberrant sister chromatid cohesion in primary HeH ALL, and how it may affect chromosomal heterogeneity within the HeH subgroup. We found that primary HeH frequently have severe cohesion defects in metaphase chromosomes that are associated with increased chromosomal copy number heterogeneity, indicating that a subset of HeH ALL may possibly harbor CIN. Our data point to a novel opportunity for targeted therapy in HeH ALL, in line with other cancers with cohesion defects.

2 | MATERIALS AND METHODS

2.1 | Patient samples

Eighty-two childhood ALL cases were included in the study (Supporting Information Table S1), selected on the basis of material being available. Forty-five cases displayed HeH as ascertained by G-banding, fluorescence in situ hybridization (FISH) and/or single nucleotide polymorphism (SNP) array analysis, whereas 37 were *ETV6/RUNX1*-positive by reverse transcriptase quantitative PCR (RT-PCR) and/or FISH. We have

previously shown that the latter generally display normal levels of cohesin.¹⁰ Diagnostic samples obtained at ALL diagnosis and stored in fixative (methanol:acetic acid, 3:1) for 1 to 31 years were utilized. Informed consent was obtained according to the Declaration of Helsinki and the study was approved by the Ethics Committee of Lund University. SNP array data from samples obtained at diagnosis were available for all cases except HeH_29 and have been previously published.^{3,4} These data were reanalyzed to identify subclonal chromosome gains using TAPS.²⁹ The lower limit of detecting subclonality using this technique was estimated to be approximately 10% to 20% of the cells.

2.2 | *RAD21* knockdown

To investigate the effect of lower levels of cohesin, we performed shRNA-mediated knockdown of *RAD21* (*RAD21*-KD) in the *ETV6/RUNX1*-positive ALL REH cell line (ACC-22, DSMZ, Braunschweig, Germany) according to methods previously described.²⁶ Briefly, lentivirus carrying the shRNA construct and expressing GFP were produced using the human cell line 293 T.^{26,30} REH cells were cultured in standard cell medium (RPMI, 20% FBS, 1% P/S) and transduction was done with two different shRNAs targeting *RAD21* (*RAD21* shRNA-1 and *RAD21* shRNA-2, respectively) as well as a non-targeting shRNA control, with three replicates for each. GFP+ cells were sorted by FACS 48 hours post-transduction. Gene expression levels were determined 1 week after transduction by RT-PCR (7500 Real-Time PCR system; Applied Biosystems, Waltham, MS), using probes from Taqman (Life Technologies, Carlsbad, CA) for *RAD21* (Hs00366721_mH) and *HPRT1* (Hs02800695_m1). Cytogenetic analysis was performed according to standard methods 2 to 3 and immunofluorescence 4 to 5 weeks post-transduction.

2.3 | Cohesion assay

Sister chromatid cohesion assay was performed according to Sajesh et al¹⁵ in the *RAD21*-KD REH cells and controls (blinded analysis) and in the primary patient samples. For the latter, the analysis was done without prior knowledge of expression levels of members of the cohesin or condensin complexes. FISH or standard G-banding preparations were analyzed using a Z2 fluorescence microscope (Zeiss, Oberkochen, Germany). Images were captured and enhanced using the CytoVision software (Leica, Wetzlar, Germany). Aberrant cohesion was defined as the presence of primary constriction gaps (PCGs), that is, visible gaps between the sister chromatids at the centromeres.¹⁵ The severity of PCGs was classified based on literature,¹⁵ with the addition of a fourth category: (a) PCG-I (mild), 1-4 chromosomes with PCGs; (b) PCG-II (moderate) 5-19 chromosomes with PCGs; (c) PCG-III (severe) ≥ 20 chromosomes with PCGs, but not all; and (d) PCG-IV (very severe), complete loss of cohesion. Since *ETV6/RUNX1* is cryptic, leukemic blasts were identified by simultaneous detection of the translocation by FISH or by additional chromosomal aberrations identifiable by chromosome banding. The frequency of cohesion defects in the different subgroups was compared using the Mann-Whitney

U test; *P*-values <.05 were considered significant. Furthermore, the overall frequency of chromosomes with cohesion defects per patient was calculated taking the number of chromosomes with cohesion defects and dividing it by the total number of chromosomes times the number of analyzed cells.¹⁵

2.4 | Immunofluorescence

The frequency of aberrant mitoses in REH cells under *RAD21* knock-down was investigated in a blinded manner using the *RAD21*-KD cells and controls. Slide preparation was performed according to the guidelines “Cell Staining for Immunofluorescence Microscopy” provided by BD Biosciences (Franklin Lakes, NJ), with minor modifications. A minimum of 100 mitoses were analyzed for each replicate, and statistical significance was evaluated by the Mann-Whitney *U* test; *P*-values <.05 were considered significant. Primary antibodies anti-tubulin alpha (produced in rabbit, SAB4500087; Sigma-Aldrich, St. Louis, MO) and anti-tubulin gamma (produced in mouse, T6557; Sigma-Aldrich) were used to label microtubuli and centrosomes, respectively. Samples were counterstained with anti-rabbit IgG (FITC green, F1262; Sigma-Aldrich) and anti-mouse IgG (Cy3 orange, C2181; Sigma-Aldrich) and slides were mounted with Vectashield medium with DAPI (H-1200; Vector Laboratories, Burlingame, CA).

2.5 | Interphase FISH

Interphase FISH was done in a blinded manner on *RAD21*-KD cells and controls according to standard methods. Slides from each replicate were hybridized with FISH probes for chromosomes X, 2, 3 and 21 (Vysis, Abbott Laboratories, Chicago, IL). A total of 300 nuclei were analyzed for each replicate, with each probe counted separately. Interphase FISH on HeH primary samples was done in a blinded manner in >300 nuclei in five cases with high percentage and five cases with low percentage of cohesion defects, all chosen according to availability of material, using probes for chromosomes X, 2, 3, 6, 10, and 21 (Vysis). To minimize technical artefacts, only cases with the same copy number for the analyzed chromosome in the major clone were included in each analysis. To ensure that only leukemic blasts were analyzed, only nuclei where the other probes confirmed hyperdiploidy were included.

2.6 | Gene expression correlation

Data from RNA-sequencing were available for 36 of the HeH and 32 *ETV6/RUNX1*-positive cases (Supporting Information Table S1).³¹ For each cohesin- and condensin-related gene, HeH cases were divided into two groups: high expression and low expression (top and bottom 50% of cases for the given gene); one-sided Mann-Whitney *U* test was applied to inquire whether the low expression groups presented higher levels of cohesion defects. Genes included in the analysis were core subunits of the cohesin and condensin complexes, that is,

RAD21, *SMC1A*, *SMC3*, *STAG1*, *STAG2* (cohesin), *NCAPD2*, *NCAPD3*, *NCAPG*, *NCAPG2*, *NCAPH*, *NCAPH2*, *SMC2* and *SMC4* (condensin I and II); *P* < .05 was considered significant.

3 | RESULTS

3.1 | Primary patient samples of HeH ALL have aberrant sister chromatid cohesion

To investigate whether primary ALL samples display cohesion defects, we first ensured that we could detect cohesion defects by analyzing the *RAD21*-knockdown cells (2 to 2.5-fold decrease in *RAD21* expression; Supporting Information Figure S1). The proportion of mitotic cells displaying cohesion defects was clearly higher in *RAD21*-knockdown cells: 36% and 33%, respectively, of two technical replicates vs 4% of control cells (*P* = 0.0119, Mann-Whitney *U* test; Supporting Information Figure S2A-B and Table S2). *RAD21*-KD cells also displayed more severe defects, ranging from PCG I-III, while controls presented only PCG I (Supporting Information Table S2). These results are in line with previous reports of cohesin knockdown,^{14,16} and shows that our analysis is able to detect sister chromatid cohesion defects.

Cohesion defects were detected in 86% of HeH cases vs 49% of *ETV6/RUNX1*-positive cases (*P* = 3.02×10^{-8} ; Mann-Whitney *U* test; Figure 1, Supporting Information Table S3). In HeH cases, 0% to 85% of the cells displayed cohesion defects (Figure 1E), with mild defects (PCG I) seen in 27%, moderate defects (PCG II) in 40%, and severe defects (PCG III) in 11% of cases (Figure 1). Complete loss of cohesion was observed in two cells from case HeH_14 and in one cell each from cases HeH_18 and HeH_45 (7% of cases). In *ETV6/RUNX1*-positive cases, cohesion defects were seen in 0% to 18% of cells, with 30% of cases classified as mild, 14% as moderate and 5% as severe. Complete loss of cohesion was not observed. Taken together, the distribution between the categories (PCG I-PCG IV) clearly differed between the two subtypes (Figure 1F). Furthermore, the frequency of chromosomes displaying cohesion defects per case (based on each case's modal chromosome number) was significantly higher in HeH ALL than in *ETV6/RUNX1*-positive ALL (*P* = 4.74×10^{-8} , Mann-Whitney *U* test; Supporting Information Table S3). Remission samples from twelve HeH and eight *ETV6/RUNX1*-positive cases were also analyzed to investigate the frequency of cohesion defects in normal cells. Of 210 analyzed normal cells, only one cell in one remission sample had mild cohesion defects (0.48%). Thus, sister chromatid cohesion defects were both significantly more common and more severe in primary HeH as compared with primary *ETV6/RUNX1*-positive ALL and normal bone marrow cells.

3.2 | Cohesion defects are associated with increased chromosomal heterogeneity in primary HeH ALL

Next, we investigated whether cohesion defects lead to increased chromosomal heterogeneity, which is indicative of CIN, in primary

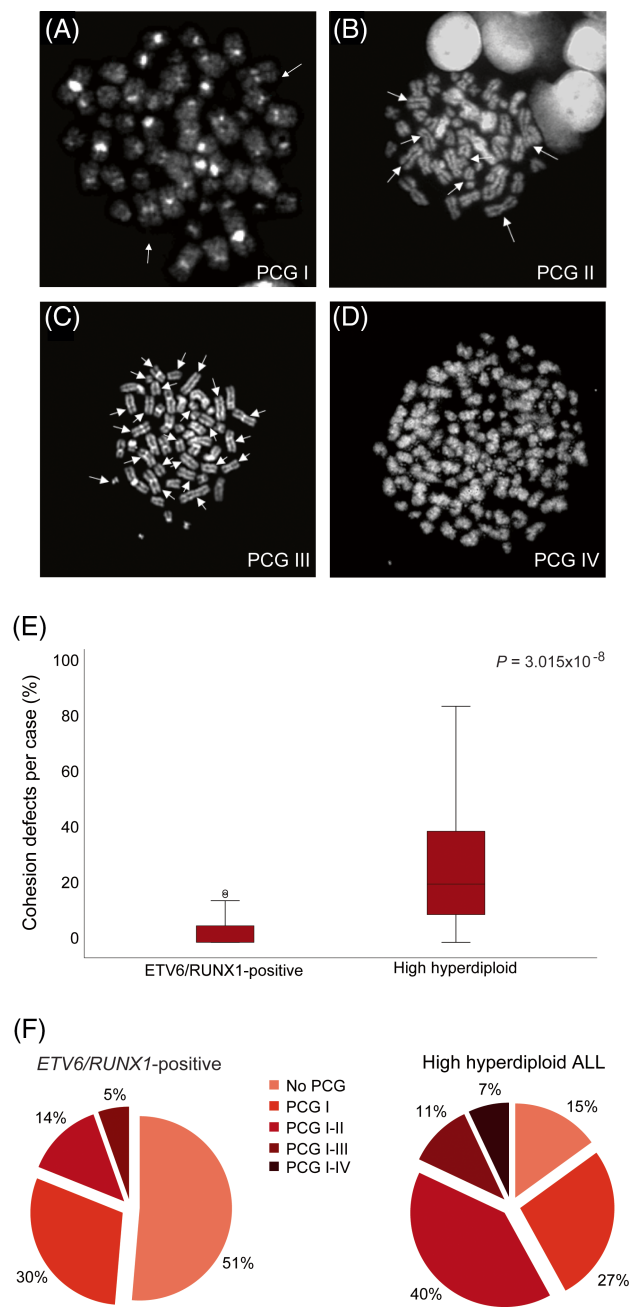


FIGURE 1 Analysis of sister chromatid cohesion, detected as primary constriction gaps (PCGs), in primary patient samples from high hyperdiploid and *ETV6/RUNX1*-positive ALL cases. A, Metaphase from case HeH_3, classified as PCG I, where two chromosomes (arrows) displayed cohesion defects; B, metaphase from case HeH_40, classified as PCG II, where seven chromosomes (arrows) displayed cohesion defects; C, metaphase from case HeH_26, classified as PCG III, where 22 chromosomes (arrows) displayed cohesion defects; D, metaphase from case HeH_14, classified as PCG IV, that is, complete loss of cohesion. E, Incidence of cohesion defects, comparing high hyperdiploid and *ETV6/RUNX1*-positive ALL cases: cohesion defects, shown as percentage of total cells presenting PCGs per case, where the boxes show the interquartile range and median (line) values, whiskers show minimum and maximum values in the cohort and outliers are shown as circles; F, classification of *ETV6/RUNX1*-positive and high hyperdiploid cases according to the cohesion assay criteria, from “no PCG” to “PCG I-IV”

ALL by interphase-FISH. There was an increase in copy number variation for all the six assessed chromosomes in cases with high levels of cohesion defects, being statistically significant for chromosomes 3, 6, 10 and 21 ($P = .0357$, $P = .00794$, $P = .0286$, and $P = .0179$, respectively; Figure 2, Supporting Information Table S4). Thus, sister chromatid cohesion defects were associated with increased chromosomal copy number heterogeneity in HeH ALL, indicating that cohesion defects may lead to increased CIN.

To investigate whether sister chromatid cohesion defects were also associated with the number of subclones involving whole chromosomes in primary HeH ALL, SNP array data was analyzed in 44 of the HeH cases. Subclonality was detected for 1 to 4 chromosomes in 18 cases (40%). No difference in the frequency of cohesion defects was seen between cases with and without subclonal chromosome changes ($P = .747$; Mann-Whitney *U* test).

3.3 | Cohesion defects are associated with decreased *RAD21* and *NCAPG* expression in primary HeH ALL

To investigate whether sister chromatid cohesion defects could be linked to cohesin or condensin levels, we analyzed whether mRNA expression of core subunits from both protein complexes correlated with the percentage of cells displaying cohesion defects. Consistent with our hypothesis, the expression of *RAD21* was negatively correlated with the number of cells displaying cohesion defects in HeH ALL ($P = .00111$; one-sided Mann-Whitney *U* test; Supporting Information Figure S3C). Moreover, low *NCAPG* levels also correlated with aberrant cohesion ($P = .00424$; one-sided Mann-Whitney *U* test; Supporting Information Figure S4C). No other correlations were seen in the HeH cases only (Supporting Information Figure S3, Supporting Information Figure S4), the *ETV6/RUNX1*-positive cases only, or in both groups combined.

3.4 | Knockdown of *RAD21* leads to increased chromosomal heterogeneity and aberrant mitoses in leukemic cells

To assess further whether the low levels of cohesin affect chromosomal stability in hematopoietic cells, we performed interphase FISH in the *RAD21*-KD cells. For all four investigated chromosomes, *RAD21*-KD cells displayed increased variation in copy number; however, it was only statistically significant for chromosome 21 (Figure 3, Supporting Information Table S5). Taken together, the interphase FISH showed increased chromosomal heterogeneity in *RAD21*-KD cells, indicating that decreased levels of cohesin lead to increased CIN.

Next, we investigated whether low expression of *RAD21* affects cell division in ALL cells by analyzing for spindle defects—monopolar, tripolar, and tetrapolar mitoses—and chromatin bridges/lagging

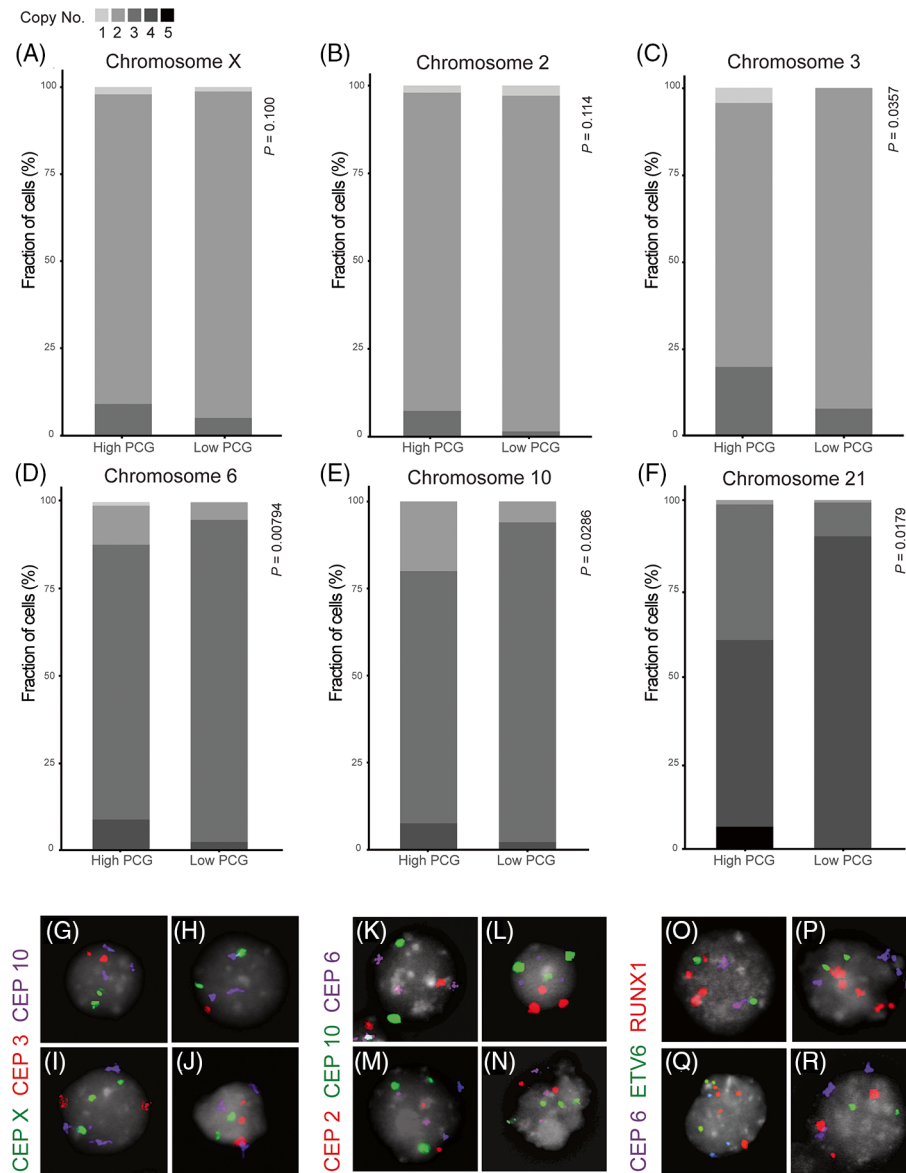
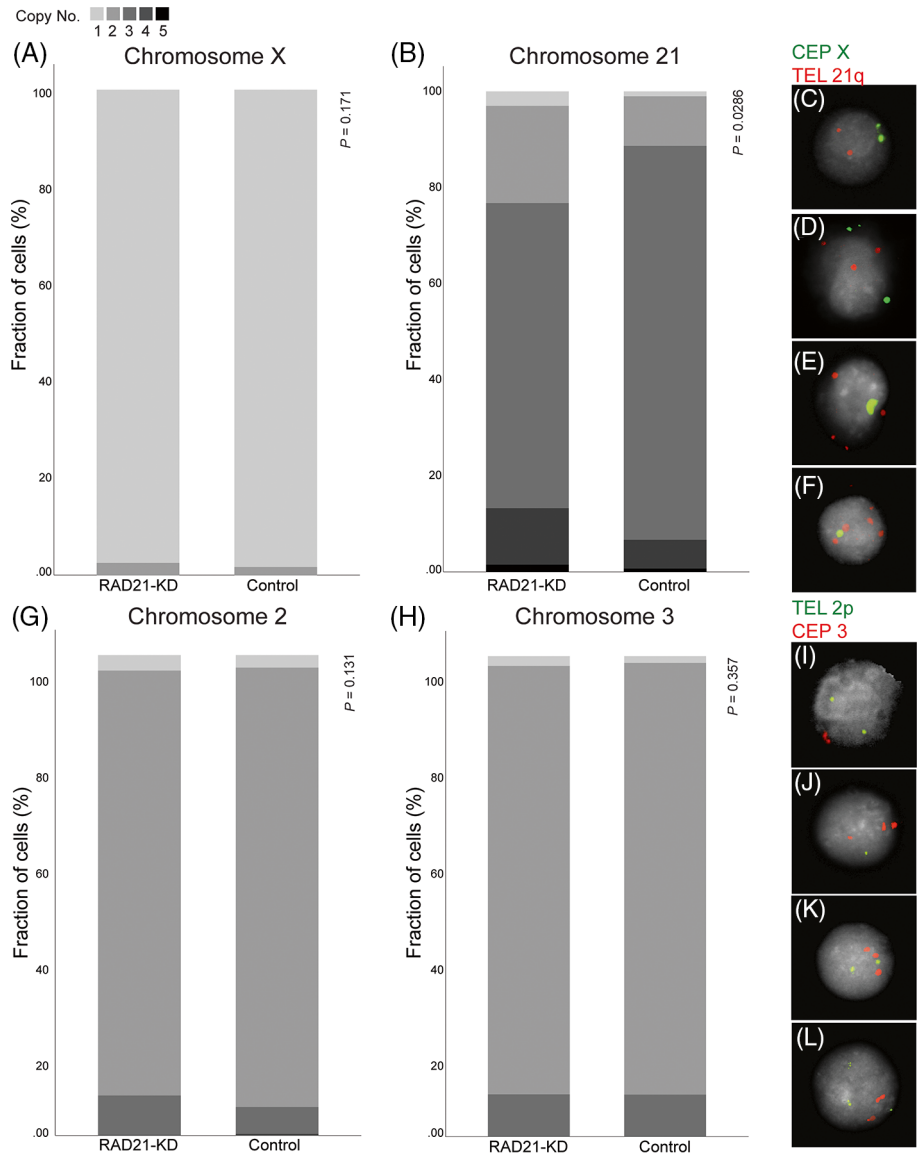


FIGURE 2 Copy number in HeH ALL primary patient cells with high PCG (primary constriction gaps) (HeH_4, HeH_14, HeH_18, HeH_40 and HeH_41) and low PCG (HeH_21, HeH_23, HeH_30, HeH_39 and HeH_42), analyzed by interphase fluorescence in situ hybridization for chromosomes X, 2, 3, 6, 10 and 21. A, Overall copy number of chromosome X, disomy expected; B, overall copy number of chromosome 2, disomy expected; C, overall copy number of chromosome 3, disomy expected; D, overall copy number of chromosome 6, trisomy expected; E, overall copy number of chromosome 10, trisomy expected; F, overall copy number of chromosome 21, tetrasomy expected; G, nucleus from HeH_42, showing disomy of chromosome X, disomy 3 and trisomy 10; H, nucleus from HeH_14, showing disomy X, monosomy 3 and trisomy 10; I, nucleus from HeH_40, showing trisomy X, disomy 3 and trisomy 10; J, nucleus from HeH_14, showing disomy X, trisomy 3 and trisomy 10; K, nucleus from HeH_14, showing monosomy 2, trisomy 6 and disomy 10; L, nucleus from HeH_41, showing trisomy 2, trisomy 6 and trisomy 10; M, nucleus from HeH_30, showing disomy 2, tetrasomy 6 and trisomy 10; N, nucleus from HeH_30, showing disomy 2, trisomy 6 and tetrasomy 10; O, nucleus from HeH_18, showing disomy 6, two copies of *ETV6* (chromosome 12) and four copies of *RUNX1* (chromosome 21); P, nucleus from HeH_40, showing tetrasomy 6, two copies of *ETV6* and five copies of *RUNX1*; Q, nucleus from HeH_18, showing trisomy 6, three copies of chromosome *ETV6* and five copies of *RUNX1*; R, nucleus from HeH_40, showing trisomy 6, two copies of *ETV6* and three copies of *RUNX1*

chromosomes (Supporting Information Figure S2C-F, Table S6). The overall frequency of mitotic aberrations in RAD21-KD cells was 6.5%, while no control cells had such aberrations ($P = .0119$, Mann-Whitney U test; Supporting Information Figure S2G). Spindle defects were detected in 4.8% of RAD21-KD cells; in particular, tripolar mitoses

were more frequent ($P = .0119$; Mann-Whitney U test). Chromatin bridges/lagging chromosomes were only seen in RAD21-KD cells (1.6% of the cells). Taken together, lower expression of RAD21 increased the frequency of spindle defects, in particular tripolar mitoses.

FIGURE 3 Copy number in REH cells with low expression of RAD21 (RAD21-KD cells) and controls, analyzed by interphase fluorescence in situ hybridization for chromosomes X, 2, 3 and 21. A, Overall copy number of chromosome X, monosomy expected; B, overall copy number of chromosome 21, trisomy expected; C, nucleus from replicate RAD21.1-3, showing one copy of chromosome X and two copies of chromosome 21; D, nucleus from replicate RAD21.2-3, showing two copies of chromosome X and three copies of chromosome 21; E, nucleus from replicate RAD21.2-2, showing one copy of chromosome X and four copies of chromosome 21; F, nucleus from replicate RAD21.1-3, showing one copy of chromosome X and five copies of chromosome 21; G, overall copy number of chromosome 2, disomy expected; H, overall copy number of chromosome 3, disomy expected; I, nucleus from replicate RAD21.2-4, showing two copies of chromosome 2 and one copy of chromosome 3; J, nucleus from replicate RAD21.2-5, showing one copy of chromosome 2 and three copies of chromosome 3; K, nucleus from replicate control 5, showing two copies of chromosome 2 and three copies of chromosome 3; L, nucleus from replicate control 5, showing two copies of chromosome 2 and two copies of chromosome 3



4 | DISCUSSION

In this study, we found that HeH ALL cells frequently harbor aberrant cohesion, in line with the recent investigation by Molina et al.²⁸ In a further expansion of their findings, we report that the incidence and severity of defects vary within the subgroup. HeH ALL displayed both a higher frequency and more severe cohesion defects compared to *ETV6/RUNX1*-positive cases. Notably, the percentage of aberrant cohesion ranged from 0% to 85% in primary HeH ALL, where 40% of the cases presented moderate and 18% presented severe or very severe cohesion defects, showing that aberrant sister chromatid cohesion is a widespread, yet heterogeneous, phenomenon in HeH childhood ALL.

Sister chromatid cohesion defects may be associated with CIN, which in turn may give rise to increased heterogeneity in chromosomal copy numbers. Whether HeH ALL display CIN or not is a controversial issue. Some investigators have reported widespread chromosomal heterogeneity when using interphase FISH to analyze

commonly gained chromosomes.^{28,32-34} However, a major problem with these studies is that they have compared HeH samples containing trisomies with normal or other BCP ALL samples containing disomies. Since the baseline number of the chromosomes differ between these two groups, appropriate cut-off levels for the probes cannot be determined and solid data are thus lacking. Here, we circumvented this problem by comparing two groups of HeH cases, only including cases with the same copy number for the analyzed chromosomes. We detected a clear difference between cases with high levels of sister chromatid cohesion defects and those with low levels/no cohesion defects. Thus, we can conclude that aberrant sister chromatid cohesion result in increased levels of chromosomal copy number heterogeneity. Although the link between chromosomal copy number heterogeneity and CIN is not absolute, these findings suggest that cohesion defects are associated with increased CIN. However, this did not translate into an increased number of subclones detectable by SNP array analysis in cases with high levels of cohesion defects, likely due to the lower limit of detection of subclonal trisomies with this

method being approximately 10-20%, preventing detection of smaller subclones. Molina et al²⁸ reported that inhibition of AURKB, suggested to be the functional outcome of defective condensin in their study, in CD34-positive hematopoietic stem/progenitor cells led to an increase in the number of hyperdiploid cells, although no further characterization of the exact chromosomal content of these cells was done. However, considering that we show that not all HeH cases display cohesion defects, regardless of the underlying cause, it does seem unlikely that these are directly causative of the aneuploidy, in particular as the allelic patterns in HeH ALL suggest that the majority of extra chromosomes are gained in one abnormal cell division.³⁵⁻³⁷ Rather, sister chromatid cohesion defects may promote clonal evolution in HeH ALL through increased chromosomal heterogeneity. Taken together, since the incidence of cohesion defects as well as the level of chromosomal heterogeneity varies among HeH cases, these phenomena are likely not early events in leukemogenesis, but could rather have a role in later optimization of the chromosomal gains once the initial hyperdiploidy has been established.

We recently reported that HeH ALL display low levels of cohesin compared to *ETV6/RUNX1*-positive cases and normal BCP cells.¹⁰ This was shown on the protein level as well in multiple mRNA datasets and impacted the overall gene expression. Since low cohesin levels would be expected to also result in aberrant cohesion, we investigated whether the cohesion defects described here in primary HeH ALL correlated with the expression of cohesin subunits in HeH ALL. We found a negative correlation between *RAD21* mRNA expression and the incidence of cohesion defects, in agreement with prior *in vitro* studies,^{14,15} whereas no statistically significant correlation was seen for the remaining genes. Another recent study investigated the incidence of mitotic and chromosomal defects in HeH ALL compared to other B-ALL subgroups, suggesting that impairment of aurora B kinase and the condensin complex were underlying such abnormalities.²⁸ Although the authors observed no correlation at the mRNA expression level of condensin, suggesting that posttranslational modifications were likely to be the cause of condensin impairment, we here found that *NCAPG* mRNA expression correlates with cohesion defects within the HeH ALL subgroup. Taken together, we cannot definitely state whether dysregulation of cohesin, condensin, or a combination of both causes cohesion defects in primary ALL.

There are conflicting data in the literature on the link between cohesin dysregulation and aneuploidy. Solomon et al^{18,25} reported increased variability in chromosome numbers in cell lines with knockdown of *STAG2*, whereas Balbás-Martínez et al³⁸ did not observe such effects. Using interphase FISH, we detected increased chromosomal heterogeneity for chromosome 21, the only investigated trisomy, in REH leukemic cells with knockdown of *RAD21*, but not for chromosomes X, 2 and 3. Whether this discrepancy is due to an underlying chromosome-specific effect—as recently shown to exist for certain CIN-associated phenomena³⁹—or to the fact that more copy number variation can be expected for trisomic chromosomes, simply because there are more copies that can be affected, remain to be investigated. Taken together, our data support that low expression

of *RAD21* compromises the integrity of chromosome segregation in BCP ALL cells, at least for some chromosomes.

Recent studies have suggested possible agents for targeted therapy in cohesion-defective cancers, based on synthetic lethality experiments in cells with aberrant cohesion. In particular, inhibition of the anaphase promoting complex in the presence of aberrant cohesion has been shown to have synthetic lethality, leading to mitotic death.⁴⁰ Furthermore, synthetic lethality has been described for cohesin defects and poly-ADP ribose polymerases (PARP)—a protein involved in double-stranded DNA repair—where cell lines under siRNA-mediated depletion of *SMC1*, *SMC3* or *RAD21* showed increased sensitivity to the PARP-inhibitor olaparib.⁴¹ Thus, considering our data showing that primary samples have cohesion defects, such treatments could be a possible future option in at least a subset of HeH ALL.

CONFLICT OF INTEREST

The authors declare no potential conflicts of interest.

DATA AVAILABILITY STATEMENT

The RNA dataset used in this study is available at the European Genome-phenome archive under accession number EGAD00001002112. SNP array data are not publicly available due to privacy concerns but are available from the corresponding author on reasonable request.

ORCID

Larissa H. Moura-Castro  <https://orcid.org/0000-0001-9063-5592>

Pablo Peña-Martínez  <https://orcid.org/0000-0002-0789-6431>

Kajsa Paulsson  <https://orcid.org/0000-0001-7950-222X>

REFERENCES

1. Soto M, Raaijmakers JA, Medema RH. Consequences of genomic diversification induced by segregation errors. *Trends Genet.* 2019;35(4):279-291.
2. Paulsson K, Johansson B. High hyperdiploid childhood acute lymphoblastic leukemia. *Genes Chromosomes Cancer.* 2009;48:637-660.
3. Davidsson J, Paulsson K, Lindgren D, et al. Relapsed childhood high hyperdiploid acute lymphoblastic leukemia: presence of preleukemic ancestral clones and the secondary nature of microdeletions and RTK-RAS mutations. *Leukemia.* 2010;24(5):924-931.
4. Olsson L, Lundin-Strom KB, Castor A, et al. Improved cytogenetic characterization and risk stratification of pediatric acute lymphoblastic leukemia using single nucleotide polymorphism array analysis: a single center experience of 296 cases. *Genes Chromosomes Cancer.* 2018;57(11):604-607.
5. Szczepański T, Willems MJ, Van Dongen JJM, et al. Precursor-B-ALL with DH-JH gene rearrangements have an immature immunogenotype with a high frequency of oligoclonality and hyperdiploidy of chromosome 14. *Leukemia.* 2001;15(9):1415-1423.
6. Raimondi SC, Pui CH, Hancock ML, Behm FG, Filatov L, Rivera GK. Heterogeneity of hyperdiploid (51-67) childhood acute lymphoblastic leukemia. *Leukemia.* 1996;10(2):213-224.
7. Bateman CM, Alpar D, Ford AM, et al. Evolutionary trajectories of hyperdiploid ALL in monozygotic twins. *Leukemia.* 2015;29(1):58-65.
8. Yang JJ, Bhojwani D, Yang W, et al. Genome-wide copy number profiling reveals molecular evolution from diagnosis to relapse in childhood acute lymphoblastic leukemia. *Blood.* 2008;112(10):4178-4183.

9. Mullighan CG, Phillips LA, Su X, et al. Genomic analysis of the clonal origins of relapsed acute lymphoblastic leukemia. *Science*. 2008;322(5906):1377-1380.
10. Yang M, Vesterlund M, Siavelis I, et al. Proteogenomics and hi-C reveal transcriptional dysregulation in high hyperdiploid childhood acute lymphoblastic leukemia. *Nat Commun*. 2019;10(1):1519.
11. Nasmyth K. Cohesin: a catenase with separate entry and exit gates? *Nat Cell Biol*. 2011;13(10):1170-1177.
12. Morales C, Losada A. Establishing and dissolving cohesin during the vertebrate cell cycle. *Curr Opin Cell Biol*. 2018;52(9):51-57.
13. Kaur M, DeScipio C, McCallum J, et al. Precocious sister chromatid separation (PSCS) in Cornelia de Lange syndrome. *Am J Med Genet A*. 2005;138A(1):27-31.
14. Losada A, Yokochi T, Hirano T. Functional contribution of Pds5 to cohesin-mediated cohesion in human cells and *Xenopus* egg extracts. *J Cell Sci*. 2005;118(10):2133-2141.
15. Sajesh BV, Lichtensztejn Z, McManus KJ. Sister chromatid cohesion defects are associated with chromosome instability in Hodgkin lymphoma cells. *BMC Cancer*. 2013;13(1):391.
16. Stoecker C, Ameziane N, van der Lelij P, et al. Defects in the Fanconi anemia pathway and chromatid cohesion in head and neck cancer. *Cancer Res*. 2015;75(17):3543-3553.
17. Barber TD, McManus K, Yuen KWY, et al. Chromatid cohesion defects may underlie chromosome instability in human colorectal cancers. *Proc Natl Acad Sci U S A*. 2008;105(9):3443-3448.
18. Solomon DA, Kim T, Diaz-Martinez LA, et al. Mutational inactivation of STAG2 causes aneuploidy in human cancer. *Science*. 2011;333(6045):1039-1043.
19. Kleymann M, Kabeche L, Compton DA. STAG2 promotes error correction in mitosis by regulating kinetochore-microtubule attachments. *J Cell Sci*. 2014;127(19):4225-4233.
20. Hoque MT, Ishikawa F. Cohesin defects lead to premature sister chromatid separation, kinetochore dysfunction, and spindle-assembly checkpoint activation. *J Biol Chem*. 2002;277(44):42306-42314.
21. Toyoda Y, Yanagida M. Coordinated requirements of human topo II and cohesin for metaphase centromere alignment under Mad2-dependent spindle checkpoint surveillance. *Mol Biol Cell*. 2006;17(5):2287-2302.
22. Watrin E, Schleiffer A, Tanaka K, Eisenhaber F, Nasmyth K, Peters JM. Human Scc4 is required for cohesin binding to chromatin, sister-chromatid cohesion, and mitotic progression. *Curr Biol*. 2006;16(9):863-874.
23. Yan J, Enge M, Whittington T, et al. Transcription factor binding in human cells occurs in dense clusters formed around cohesin anchor sites. *Cell*. 2013;154(4):801-813.
24. Lawrence MS, Stojanov P, Mermel CH, et al. Discovery and saturation analysis of cancer genes across 21 tumour types. *Nature*. 2014;505(7484):495-501.
25. Solomon DA, Kim J-S, Bondaruk J, et al. Frequent truncating mutations of STAG2 in bladder cancer. *Nat Genet*. 2013;45(12):1428-1430.
26. Galeev R, Baudet A, Kumar P, et al. Genome-wide RNAi screen identifies cohesin genes as modifiers of renewal and differentiation in human HSCs. *Cell Rep*. 2016;14(12):2988-3000.
27. Fisher JB, McNulty M, Burke MJ, Crispino JD, Rao S. Cohesin mutations in myeloid malignancies. *Trends Cancer*. 2017;3(4):282-293.
28. Molina O, Vinyoles M, Granada I, et al. Impaired condensin complex and Aurora B kinase underlie mitotic and chromosomal defects in hyperdiploid B-cell ALL. *Blood*. 2020;136(3):313-327.
29. Rasmussen M, Sundstrom M, Goransson Kultima H, et al. Allele-specific copy number analysis of tumor samples with aneuploidy and tumor heterogeneity. *Genome Biol*. 2011;12(10):R108.
30. Ali N, Karlsson C, Aspling M, et al. Forward RNAi screens in primary human hematopoietic stem/progenitor cells. *Blood*. 2009;113(16):3690-3695.
31. Lilljebjorn H, Henningsson R, Hyrenius-Wittsten A, et al. Identification of ETV6-RUNX1-like and DUX4-rearranged subtypes in paediatric B-cell precursor acute lymphoblastic leukaemia. *Nat Commun*. 2016;7(1):11790.
32. Betts DR, Riesch M, Grotzer MA, Niggli FK. The investigation of karyotypic instability in the high-hyperdiploidy subgroup of acute lymphoblastic leukemia. *Leuk Lymphoma*. 2001;42(1-2):187-193.
33. Blandin AT, Muhlematter D, Bougeon S, et al. Automated four-color interphase fluorescence in situ hybridization approach for the simultaneous detection of specific aneuploidies of diagnostic and prognostic significance in high hyperdiploid acute lymphoblastic leukemia. *Cancer Genet Cytogenet*. 2008;186(2):69-77.
34. Alpar D, Pajor G, Varga P, et al. Sequential and hierarchical chromosomal changes and chromosome instability are distinct features of high hyperdiploid pediatric acute lymphoblastic leukemia. *Pediatr Blood Cancer*. 2014;61(12):2208-2214.
35. Onodera N, McCabe NR, Rubin CM. Formation of a hyperdiploid karyotype in childhood acute lymphoblastic leukemia. *Blood*. 1992;80(1):203-208.
36. Paulsson K, Panagopoulos I, Knuutila S, et al. Formation of trisomies and their parental origin in hyperdiploid childhood acute lymphoblastic leukemia. *Blood*. 2003;102(8):3010-3015.
37. Paulsson K, Morse H, Fioretos T, et al. Evidence for a single-step mechanism in the origin of hyperdiploid childhood acute lymphoblastic leukemia. *Genes Chromosomes Cancer*. 2005;44(2):113-122.
38. Balbas-Martinez C, Sagrera A, Carrillo-de-Santa-Pau E, et al. Recurrent inactivation of STAG2 in bladder cancer is not associated with aneuploidy. *Nat Genet*. 2013;45(12):1464-1469.
39. Worrall JT, Tamura N, Mazzagatti A, et al. Non-random mis-segregation of human chromosomes. *Cell Rep*. 2018;23(11):3366-3380.
40. de Lange J, Faramarz A, Oostra AB, et al. Defective sister chromatid cohesion is synthetically lethal with impaired APC/C function. *Nat Commun*. 2015;6(1):8399.
41. McLellan JL, O'Neil NJ, Barrett I, et al. Synthetic lethality of cohesins with PARPs and replication fork mediators. *PLoS Genet*. 2012;8(3):e1002574.

SUPPORTING INFORMATION

Additional supporting information may be found online in the Supporting Information section at the end of this article.

How to cite this article: Moura-Castro LH, Peña-Martínez P, Castor A, et al. Sister chromatid cohesion defects are associated with chromosomal copy number heterogeneity in high hyperdiploid childhood acute lymphoblastic leukemia. *Genes Chromosomes Cancer*. 2021;60:410-417. <https://doi.org/10.1002/gcc.22933>